npj Parkinson's Disease

https://doi.org/10.1038/s41531-026-01291-1

Article in Press

Free water in the external globus pallidus predicts mild cognitive impairment in Parkinson's disease and is associated with serum neurofilament light chain levels

Received: 21 September 2025

Accepted: 3 February 2026

Cite this article as: Chen, H., Liu, H., Kou, W. *et al.* Free water in the external globus pallidus predicts mild cognitive impairment in Parkinson's disease and is associated with serum neurofilament light chain levels. *npj Parkinsons Dis.* (2026). https://doi.org/10.1038/s41531-026-01291-1

Huimin Chen, Huijing Liu, Wenyi Kou, Xinxin Ma, Yunfei Long, Dongdong Wu, Wei Du, Jing He, Shuhua Li, Haibo Chen & Wen Su

Free water in the external globus pallidus predicts mild cognitive impairment in Parkinson's disease and is associated with serum neurofilament light chain levels

Huimin Chen[1], Huijing Liu[1], Wenyi Kou[1], Xinxin Ma[1], Yunfei Long[1], Dongdong Wu[1], Wei Du[1], Jing He[1], Shuhua Li[1], Haibo Chen[1], Wen Su[1*]

[1] Department of Neurology, Beijing Hospital, National Center of Gerontology, Institute of Geriatric Medicine, Chinese Academy of Medical Sciences, Beijing, China.

Corresponding author: Wen Su, MD.

Department of Neurology, Beijing Hospital, National Center of Gerontology, Institute of Geriatric Medicine, Chinese Academy of Medical Sciences, No. 1, Dongdandahua Road, Dongcheng District, Beijing 100730, China

Business Telephone: 0086-010-85136182

E-mail address: suwenbjyy@163.com

Abstract

This study explored free-water diffusion tensor imaging (FW-DTI) in basal ganglia as a biomarker for mild cognitive impairment (MCI) in Parkinson's disease (PD). One hundred and fourteen drug-naïve PD patients (without MCI at baseline) and 102 healthy controls (HC) from Parkinson's Progression Markers Initiative (PPMI) were included, and FW-DTI metrics were extracted from the bilateral putamen, caudate, external globus pallidus (GPe), and internal globus pallidus (GPi). The result showed that PD-MCI convertors had significantly higher FW in GPe and GPi. Cox regression identified that GPe FW, MDS-UPDRS Part I score, and CSF $A\beta_{42}$/pTau were significantly associated with MCI conversion in PD during five-year follow-up. GPe FW >0.328 predicted 4.698-fold increased MCI risk (95% CI: 1.974–11.179) in PD in five years, after adjusting for CSF $A\beta_{42}$/pTau value and MDS-UPDRS part I score. Furthermore, higher GPe FW correlated with executive dysfunction (symbol digit modalities: R = -0.272, P = 0.004; letter number sequencing: R = -0.199, P = 0.035) and elevated serum neurofilament light chain (R = 0.322, P < 0.001) in PD, but not HC. In conclusion, GPe FW may serve as a sensitive imaging biomarker reflecting neuronal injury and MCI conversion risk in PD.

Keywords: Parkinson's disease; Mild cognitive impairment; Free-water diffusion tensor imaging; External globus pallidus; Neurofilament light chain

Introduction

Parkinson's disease (PD), the second most prevalent neurodegenerative disorder globally, is characterized by α-synuclein accumulation and Lewy body formation in the substantia nigra. These pathological changes are believed to drive dopaminergic network dysfunction, manifesting as motor symptoms (e.g., bradykinesia). Notably, PD is also prominently associated with non-motor symptoms, particularly cognitive impairment. An estimated 40% of PD patients develop mild cognitive impairment (MCI)[1], with approximately 80% progressing to dementia over 8 years[2]. MCI is a crucial stage of cognitive decline in PD, which serves as a transitional phase between normal cognition and PD dementia and marks a critical window for early intervention. Despite the significance and high prevalence of PD-MCI, the pathogenesis remains multifactorial and poorly understood.

Neuroimaging studies provide critical insights into the pathogenesis of cognitive impairment in PD, including PD-MCI. For instance, diffusion tensor imaging (DTI) studies demonstrated that microstructural degeneration in the cholinergic nucleus basalis of Meynert preceded overall cognitive deficits measured by the Montreal Cognitive Assessment (MoCA) as well as the development of PD-MCI[3-5]. However, conventional DTI indices have a key limitation: they model each voxel as a single tissue compartment, inherently conflating signals from actual brain tissue and extracellular free water. This limitation has been addressed by Free Water (FW) imaging, an advanced diffusion technique specifically designed to isolate and quantify the extracellular FW fraction. FW imaging has emerged as a promising biomarker in PD, sensitive to neuroinflammation and neurodegeneration[6,7]. Using this technique, elevated FW in the cholinergic nucleus basalis of Meynert has also been observed in cognitively impaired PD cohorts[8,9]. Yet, despite its potential, alterations in FW within key dopaminergic pathways, particularly the basal ganglia, remain unexplored in the context of PD cognition.

This gap is significant because cognitive impairment in PD involves complex interactions between

dopaminergic and cholinergic systems[10,11]. Crucially, the basal ganglia play a central role, integrating motivation, learning, and action selection. Dopamine transporter (DAT) imaging in pre-dementia PD patients revealed that dopaminergic deficits specifically within the caudate nucleus correlated with executive dysfunction and attentional deficits[12]. Furthermore, evidence demonstrated that levodopa modulated functional connectivity within prefrontal-basal ganglia-thalamic circuits, linking this modulation to cognitive function[11]. Supporting this, our prior work showed levodopa-induced enhancements in caudate-prefrontal cortex connectivity were associated with better cognition[13]. Collectively, these findings support a central role for basal ganglia circuitry in PD cognitive decline and warrant the potential of FW imaging to provide novel insights.

Therefore, based on the established role of the basal ganglia in PD cognition and the emerging utility of FW imaging, we hypothesize that: (1) Alterations in FW within the basal ganglia manifest early in PD, potentially predicting the development of PD-MCI; (2) These early FW changes predominantly impact executive function domains in align with the role of dopaminergic system; and (3) FW abnormalities in the basal ganglia may reflect neurodegeneration process [e.g., serum neurofilament light chain (NFL) or cerebrospinal fluid (CSF) $A\beta_{42}$/pTau]. To test this hypothesis, we utilized prospective longitudinal data from the Parkinson's Progression Markers Initiative (PPMI) with five-year follow-up. Our primary aims are: (1) To identify a potential FW-based imaging biomarker for PD-MCI localized to the basal ganglia; and (2) To elucidate the underlying neural mechanisms linking basal ganglia pathology to PD-MCI.

Results

Group comparison

A total of 112 PD patients and 100 HC were included in the current analysis (Fig. S1). PD patients were stratified into MCI convertors (n = 30) and non-convertors (n = 82). Hoehn-Yahr stage, Movement Disorder Society-Unified Parkinson's Disease Rating Scale (MDS-UPDRS) part I, part II, part III, and total scores, Geriatric Depression Scale (GDS), State-Trait Anxiety Index (STAI), University of Pennsylvania Smell Identification Test (UPSIT), Rapid eye movement sleep Behavior Disorder Screening Questionnaire (RBDSQ), Scales for Outcomes in Parkinson's disease-Autonomic (SCOPA), mean DAT uptake in the putamen and caudate, and FW values in the putamen, caudate, GPe, and GPi showed significant among-group differences (Table 1-2).

Compared with non-converting MCI patients, PD-MCI convertors exhibited a significantly higher FW value in the GPi, along with a trend toward significantly lower CSF $A\beta_{42}$/pTau values and higher FW values in the putamen and GPe using ANOVA and post hoc analysis (LSD corrected) (Table 2, Fig. 1).

Notably, conventional DTI parameters—FA, MD, RD, and AD—showed no significant differences between PD-MCI convertors and non-convertors (Table S1). This finding indicated that the observed FW alterations were distinct and not attributable to changes in conventional DTI metrics.

Predictors of PD-MCI conversion by Cox regression

Parameters with P values ≤ 0.1 in the among-group comparison in Table 1 and Table 2 were entered into a Cox regression model using backward selection, which initially included standardized (z-transformed) age, Hoehn-Yahr stage, MDS-UDPRS part I, part II, part III, and total score, GDS, STAI, UPSIT, RBDSQ, SCOPA, mean DAT caudate uptake, mean DAT putamen uptake, CSF $A\beta_{42}$/pTau ratio, FW values in putamen, caudate, GPe, and GPi. The resulting model retained only three significant predictors of MCI conversion over five years in PD:

CSF $A\beta_{42}$/pTau ratio, GPe FW value, and MDS-UPDRS Part I scores (Table S2). In patients with PD, GPe FW showed no significant correlation with the CSF $A\beta_{42}$/pTau ratio (R = -0.025, P =0.808) or MDS-UPDRS Part I scores (R = -0.117, P = 0.220), and VIFs demonstrated no substantial multicollinearity among predictors. To improve clinical interpretability, non-standardized, continuous GPe FW values were further dichotomized using maximally selected rank statistics, which identified 0.328 as the optimal cutoff for predicting PD-MCI conversion in PD (Fig. 2).

The final Cox model included MDS-UPDRS Part I score, CSF $A\beta_{42}$/pTau ratio, and stratified GPe FW groups. After adjusting for MDS-UPDRS Part I score and CSF $A\beta_{42}$/pTau, patients with GPe FW > 0.328 exhibited a 4.698-fold increased risk of MCI conversion (95% CI 1.974–11.179); The inclusion of GPe FW significantly improved model fit compared to the model without stratified GPe FW group (Improved $\chi^2 = 11.205$, $P_{for\ improvement} = 0.001$) (Table 3).

Correlation between GPe FW and cognitive domains at baseline

Pearson correlation analysis demonstrated that higher GPe FW value was significantly correlated with attention and working memory assessed by LNS test score (R = -0.199, P = 0.035) and processing speed assessed by Symbol Digit Modalities (SDM) (R = -0.272, P = 0.004) in PD patients, not in HC group (Fig. 3). GPe FW was not significantly correlated with overall cognitive function, memory, or visual spatial function domains in both PD patients and HC group (Fig. S2).

Correlation between GPe FW and biomarkers at baseline

In PD patients, higher GPe FW value was significantly correlated with higher serum NFL level at baseline (R = 0.322, P < 0.001); GPe FW value was not significantly correlated with CSF $A\beta_{42}$/pTau value. In HC, GPe FW value was not significantly correlated with both serum NFL and CSF $A\beta_{42}$/pTau levels (Fig. 3). Furthermore,

GPe FW was not significantly correlated with DAT caudate uptake (R = -0.085, P = 0.378) or putamen uptake (R = -0.051, P = 0.601) (not shown in figure).

Mixed linear regression for the biological significance of serum NFL

Although PD-MCI convertors and non-convertors showed nonsignificant group differences in serum NFL level at baseline, the mixed linear model in PD patients revealed a significantly higher serum NFL level in PD-MCI convertors (main effect of MCI status F = 3.884, P = 0.050) across the five-year follow-up (Table S3). The group difference remained stable throughout the five years (Fig. 4).

Sensitive analysis for site effect

To rule out the confounding effect of study site, several sensitive analyses were conducted. First, a linear mixed-effects model, treating PD groups as a fixed effect and study site as a random intercept. The mixed-effects model showed that GPe FW value was a significant predictor of MCI conversion in PD (F = 5.419, P = 0.022), while the variability between study sites did not account for total variance (0%). Second, including both study site and the site × GPe FW interaction term in the final Cox model did not alter the overall significance of the findings (Table 3). Third, a stratified Cox regression analysis by study center yielded consistent results (Table S4). Finally, partial correlation analysis adjusting for study site demonstrated that GPe FW remained significantly correlated with SDM, LNS, and serum NFL levels in PD (Table S5), in alignment with the main results.

Validation analysis by bootstrapping

We further conducted a two-step process of backward elimination (AIC-based) followed by cut-point analysis within the bootstrap framework. The final model includes CSF $A\beta_{42}$/pTau (shrunken HR = 0.962, 95% CI: 0.943–0.981, P <0.001), GPe FW (dichotomized at 0.310, shrunken HR = 2.431, 95% CI: 1.084–5.451, P =

0.031), MDS-UPDRS I (shrunken HR = 1.236, 95% CI: 1.117–1.368, P<0.001), and Hoehn-Yahr stage (shrunken HR = 3.202, 95% CI: 1.401–7.318, P = 0.006) (Table S6), following coefficient shrinkage to address overfitting (Fig. S3). Bootstrap validation (n=1000) demonstrated good discriminative ability with a C-index of 0.745, minimal optimism (0.004), and an optimism-corrected C-index of 0.749 (Fig. S4).

Discussion

The study aimed to investigate the role of FW-DTI features in the basal ganglia as a novel biomarker for PD-MCI. The main findings included: (1) higher GPe FW demonstrated a robust and independent association with an increased risk of MCI development in PD patients over a five-year follow-up period; (2) higher GPe FW value was associated with more severe executive dysfunction, measured by processing speed, and attention/working memory, which represents a core cognitive domain impaired in early PD-MCI. This correlation was observed specifically in PD patients but not in the HC group; (3) higher GPe FW value was significantly correlated with a higher serum NFL level in PD patients but not in HC group. Collectively, these results indicated that GPe FW may be a promising and sensitive imaging biomarker for predicting MCI conversion in PD, and higher GPe FW may reflect underlying neurodegeneration and neuronal injury.

First, this study underscores the pivotal role of the GPe in cognitive dysfunction during early-stage PD, particularly in executive impairment. Executive dysfunction represents the earliest manifestations of cognitive decline in PD. The basal ganglia, including the GPe, critically modulate executive functions—such as decision-making, action selection, and cognitive flexibility—through interconnected circuits with cortical and subcortical structures[14]. Within the GPe, prototypic neurons project to the parafascicular thalamus, facilitating cognitive flexibility and action initiation ('go' signals), and arkypallidal neurons provide inhibitory control ('stop' signals) via pallidostriatal projections[15]. Optimal executive function requires dynamic coordination between these 'go' and 'stop' mechanisms. In PD, dopaminergic depletion disrupts GPe-mediated inhibition and alters striatal-cortical connectivity, ultimately driving executive dysfunction[16]. Pharmacological interventions may also modulate GPe activity. Animal studies indicate that dopaminergic agonists can hyperactivate the GPe, impairing decision-making and behavioral inhibition[17]. However, our findings remain unaffected by medication confounds,

as analyses were restricted to drug-naïve patients. In addition, the correlation between GPe FW and executive function was not significant in the control group, indicating this association might be specific in PD. Collectively, this work highlights the basal ganglia—and specifically the GPe—as a neural substrate for MCI and executive deficits in PD.

Second, the study found FW-DTI may serve as a predictive biomarker for conversion to PD-MCI. Prior FW-DTI studies indicated elevated FW in the cholinergic nucleus basalis of Meynert was associated with longitudinal changes in MoCA scores in PD patients, underscoring cholinergic degeneration as a key factor in cognitive progression[3,8,9]**.** Our results emphasize the involvement of basal ganglia structures in PD cognitive impairment using FW-DTI, especially executive dysfunction, which is consistent with the pathophysiological underpinnings of PD. In fact, extensive evidence indicates that PD-related cognitive impairment may arise from the interplay between cholinergic and dopaminergic systems, with cholinergic deficits predominantly affecting domains such as language and memory, while dopaminergic alterations may more broadly influence executive functions[14]. Together with earlier FW-DTI studies[3,8,9], our results support the notion that cognitive impairment in PD may stem from dysfunction and crosstalk between both dopaminergic and non-dopaminergic systems, and further indicate that FW-DTI represents a sensitive imaging marker for cognitive decline in PD. Whether similar associations exist in other neurodegenerative disorders, such as Lewy body dementia and Alzheimer's disease, merits further investigation. Nonetheless, FW-DTI shows promise as a sensitive predictive biomarker for PD-MCI.

MCI represents a pivotal stage in the trajectory of cognitive decline in PD. PD-MCI, specifically, serves as a transitional phase between normal cognitive function and PD dementia, marking a critical window for early intervention. Longitudinal studies have demonstrated that approximately 40% of individuals with PD-MCI may

progress to dementia within 5 years, whereas 20–25% might revert to normal cognitive status over the same period[18]. Early identification and targeted intervention for PD-MCI hold promise for slowing the rate of cognitive decline, enhancing quality of life, preserving functional independence, and improving long-term prognostic outcomes. Nevertheless, effective and reliable treatment modalities for PD-MCI remain conspicuously lacking. Current research evidence suggests that interventions such as cognitive training combined with physical activity may yield benefits by strengthening neural connectivity[19]; however, findings from these studies remain inconsistent[20]. Pharmacological approaches, including rivastigmine, showed limited efficacy in halting or delaying disease progression[21,22]. Despite these challenges, PD-MCI persists as a critical stage for therapeutic intervention, and our study identifies a potential target (GPe) for neuromodulation and proposes a biomarker framework to support future therapeutic trials for PD-MCI. Whether the population can be generalized to PD dementia needs to be tested in the future.

Finally, we observed a significant correlation between GPe FW and serum NFL levels. This finding provides supportive biological concordance, as both markers are associated with broader neurodegenerative processes. The observed increase in FW signal in the GPe could be influenced by several factors. As a key node within the basal ganglia circuits affected by PD, the progression of Lewy pathology to this region could lead to reduced tissue density[23]. The subsequent expansion of the extracellular space would allow for less restricted water diffusion. Furthermore, neuroinflammation, including microglial activation and astrogliosis, is associated with vasogenic edema and increased vascular permeability. These inflammatory processes could contribute to a higher extracellular water content. The GPe has a markedly higher density of astrocytes compared to the GPi[16]. Astrocytes play a central role in neuroinflammation, and their activation can lead to cellular swelling and an increase in extracellular water content[24]. Therefore, the rich astrocytic environment of the GPe might provide a

structural basis for a more pronounced FW signal in response to the neuroinflammatory component of PD. This might explain the association of PD-MCI with FW values in the GPe rather than GPi. Serum NFL is a well-established, though nonspecific, biomarker of axonal injury and neural damage, with elevations observed across various neurological conditions[25-27]. In the context of PD, previous studies have linked serum NFL to the progression of both motor and non-motor symptoms[28,29]. Our observation that both GPe FW and serum NFL are elevated in PD-MCI convertors and correlate with each other is consistent with the interpretation that increased GPe FW may reflect underlying processes of neural injury. However, we emphasize that this correlation is modest and does not imply disease-specific causality or serve as a direct pathological validation of the FW signal. NFL is a nonspecific marker, and the precise pathological substrates contributing to elevated GPe FW remain to be fully elucidated. Future studies incorporating more specific biomarkers and histopathological correlation are needed to validate and clarify the underlying mechanisms.

This study has several strengths. First, prospective five-year follow-up within the PPMI cohort enabled robust assessment of predictive biomarkers for MCI conversion. Second, inclusion of drug naïve patients minimized the confounding effects of dopaminergic therapies on cognition and imaging metrics. Third, the correlation of GPe FW with serum NFL and the executive domain strengthened biological plausibility and mechanistic insight. Fourth, the inclusion of HC indicated the role of GPe FW in cognition might be specific to PD. This study also has several limitations. First, the relatively small sample size may result in insufficient statistical power to detect significant differences in certain parameters, such as GPi FW. Additionally, GPi FW was automatically excluded by the Cox regression model with backward selection, which may be due to multicollinearity. Therefore, a potential role of GPi in PD cognition cannot be entirely ruled out. Second, the limited availability of CSF biomarker data—particularly for CSF NFL—precluded a comprehensive assessment

of their association with GPe FW alterations. Third, within the PPMI dataset, five-year follow-up data was only available for 54 out of the 102 HC subjects; therefore, the association with MCI development in the HC group could not be reliably evaluated. However, the correlation between GPe and behavioral and biomarker measures was significant only in PD subjects but not in HC, still suggesting that the role of GPe may be specific to PD. Fourth, bi-tensor model relies on prior assumptions and ignores non-Gaussian behaviors (e.g., restricted diffusion in cellular compartments). Although previous study has validated that FW-DTI had similar accuracy with neurite orientation dispersion and density imaging (NODDI) for the differentiation between PD and atypical parkinsonism[30], future studies using multi-shell acquisition with high b-values to characterize tissue diffusion and improve free water estimation are still needed to validate our findings. Fifth, our study utilized the well-validated CSF $A\beta_{42}$/pTau181 ratio as a marker based on prior PPMI publications[31,32]. We acknowledge that this choice has limitations in light of recent biomarker advances. Specifically, plasma and CSF p-tau217 has demonstrated superior diagnostic performance in detecting AD and AD pathology[33,34]. Future studies are needed to investigate the implication of p-tau217 in MCI and its association with FW values in PD. Sixth, participant was classified as an MCI converter upon first meeting the Level II criteria at any single follow-up visit. This approach could include instances of transient cognitive fluctuation, and future studies with stricter criteria, larger sample size, and longer follow-up period are needed. Seventh, although this study's focus is on PD-specific insights, emerging evidence highlights that individual differences in cognitive decline among PD patients arise from genetic heterogeneity[35], vascular risk factors[36], and cognitive reserve[37]. Our findings should be interpreted as part of this multifactorial framework.

In conclusion, elevated GPe FW value may be a potential predictor for PD-MCI and may also offer pathophysiological processes driving cognitive dysfunction in Parkinson’s disease.

Methods

Participant

PPMI is an ongoing, multicenter, longitudinal, observational study that was initiated in 2010 (https://www.ppmi-info.org/) (NCT01141023). Patients with drug naïve PD and healthy controls (HC) were included. The specific inclusion and exclusion criteria were detailed in previous publication[38]. The PPMI study was conducted in full accordance with the international ethical standards for human research established by the Declaration of Helsinki. The PPMI study was approved by the institutional review board at each site, and participants provided written informed consent to participate. From the entire PPMI cohort, the study included 114 PD patients and 102 HC who showed no signs of MCI at baseline, all of whom had high-resolution 3D-T1 images ($1\times1\times1$ mm³) and eligible DTI data available for analysis (Fig. S1). The data utilized in this study were downloaded from the PPMI dataset in July 2025.

Clinical assessment

For cognition, overall cognitive function was measured by MoCA and four cognitive domains were evaluated as follows. The MoCA scores were adjusted for educational level according to the standard PPMI procedure. Specifically, one point was added to the total MoCA score for participants with $\leqslant$12 years of education. Memory was evaluated by Hopkins Verbal Learning Test (HVLT) Total Recall and HVLT Recognition Discrimination tests. Visuospatial function was assessed by Benton Judgment of Line Orientation test. Processing speed was assessed by SDM test. Attention and working memory were assessed by Letter Number Sequencing (LNS) and Semantic Fluency Test (animal) tests. MCI was diagnosed following the level 2 Movement Disorder Society (MDS) diagnostic criteria for PD-MCI. Patients with any two or more of the above cognitive tests >1.5 SD below the age-adjusted standardized mean at any visit were defined as MCI[39]. The

included cognitive domains and PD-MCI definition were in accordance with the previous PPMI publications[40,41].

Motor function was assessed using the MDS-UPDRS part III and Hoehn–Yahr stage. Depression and anxiety were evaluated by GDS and STAI; smell was assessed by UPSIT; Rapid eye movement sleep Behavior Disorder (RBD) was assessed by RBDSQ; Autonomic function was assessed by SCOPA scale; Impulsive behavior was evaluated by Questionnaire for Impulsive-Compulsive Disorders in PD (QUIP) scale.

DAT single-photon emission computed tomography (SPECT) imaging was acquired at PPMI imaging centers in accordance with the PPMI imaging protocol. Mean caudate and putaminal uptakes relative to uptake in the occipital area [striatal binding ratio (SBR)] using DAT-SPECT were computed. For CSF biomarkers, the concentration of α-syn in CSF samples was analyzed using an ELISA assay available commercially from BioLegend. CSF $A\beta_{42}$, total tau (tTau), and tau phosphorylated at the threonine 181 position (pTau) were analyzed at Biorepository Core laboratories at the University of Pennsylvania using Elecsys electrochemiluminescence immunoassays (Roche Diagnostics). Serum NFL level was analyzed using ELISA with Simoa NF-Light Advantage Kit[42]. Further details on the protocol, CSF and serum biomarkers, clinical variables, and imaging paradigm have been described in the previous publication[38].

MRI data acquisition

MRI images of the included subjects were acquired on 3-Tesla Siemens scanners (PD n = 114, HC n = 77), Philips scanners (HC n = 10), and GE scanners (HC n = 15). Sagittal 3D-T1 weighted images were acquired using accelerated MPRAGE sequence: TR = 2300 ms, TE = 2.98 ms, flip angle = 9°, image resolution = 1.0 × 1.0 × 1.0 mm^3, acquisition matrix = 240 × 256. DTI sequences were acquired with TR= 900 ms, TE=88 ms, flip angle =90°, voxel size 1.98 x 1.98 x 2 mm^3, slice thickness = 2 mm. There were 64 gradient directions with a b-value =1000 s/mm2, and one reference non-gradient volume (b=0 s/mm2).

DTI and free water processing

This processing step utilized MRtrix3 (https://www.mrtrix.org/, v3.0.4)[43], FSL (http://www.fmrib.ox.ac.uk/fsl/, v6.0.4), dipy (v1.7.0), and ANTs software.

For data preprocessing**,** Diffusion data were preprocessed using MRtrix3 tools for denoising, Gibbs ringing artifact correction, and motion/eddy current correction with b-vector adjustment. Notably, susceptibility-induced distortion correction (e.g., TOPUP) was not performed as reverse phase-encoded data were not acquired. N4 bias field correction was then applied using ANTs to address intensity inhomogeneities. Finally, diffusion tensor metrics [Fractional Anisotropy (FA), Mean Diffusivity (MD), Axial Diffusivity (AD), and Radial Diffusivity (RD)] were calculated using FSL's dtifit.

Then, FW map was generated by fitting a single-shell bi-tensor model using Dipy's regularized gradient descent algorithm. Initial guesses were derived from the HY hybrid model (free water signal initial value = 1500 $\mu m^2/s$, tissue signal = 200 $\mu m^2/s$). This model estimates a free-water compartment (extracellular water) and a tissue compartment (reflecting microstructure after removing the free-water contribution)[44].

A two-step registration procedure was performed using the antsRegistrationSyN.sh from ANTs software package to warp all diffusion maps (FA, MD, AD, RD, FW) from native space to the California Institute of Technology (CIT168) template space. First, the subject's FA map was registered to their skull-stripped T1-weighted image via a rigid-body transformation with a mutual information metric, correcting for inter-scan motion. Second, the T1-weighted image was normalized to the CIT168 template using a combination of affine (linear) and SyN (nonlinear, diffeomorphic) transformations for global and local anatomical alignment, respectively. The deformation fields from these two steps (FA → T1 and T1 → Template) were concatenated. The resulting composite transformation was applied to warp all diffusion metric maps into standard space. To

ensure quality, registration accuracy was assessed by qualitative visual inspection by an experienced researcher (HM Chen). All normalized FA maps were overlaid onto the CIT168 template and visually inspected to verify accurate alignment of major white matter tracts and deep gray matter structures. To quantitatively confirm registration accuracy, correlation coefficient between each individual's warped T1 image and the standard T1 template were further extracted. The correlation coefficient for all included subjects exceeded 0.95, suggesting excellent registration (Fig. S5).

Finally, mean values for each diffusion metric were extracted from the basal ganglia nuclei defined in the CIT168 Atlas [bilateral putamen, caudate, external globus pallidus (GPe), and internal globus pallidus (GPi)]. Individual ROIs were defined using FSL's fslmaths, and mean metric values within each ROI were computed using fslstats. The final value for each nucleus was reported as the mean of the left and right hemispheres.

Two patients with PD and Two HC were excluded due to excessive head motion (maximum absolute displacement greater than 3mm). No datasets were excluded due to processing failures or severe misregistration. The steps and modules in data processing were summarized in Table S7.

Statistics

Statistical analyses were conducted using SPSS 25.0 (SPSS Inc., Chicago, IL, USA) and R 4.3.3 (http://cran.r-project.org/). Categorical variables were presented as percentages; continuous variables were expressed as mean ± standard deviation (SD) or median (interquartile range), according to data distribution. Group comparisons employed χ^2 tests for categorical variables and one-way ANOVA or Kruskal-Wallis one-way ANOVA for continuous variables, as appropriate. Post-hoc analysis was conducted using Least Significant Difference (LSD) method.

Demographic, clinical, and diffusion metrics (DTI/FW) demonstrating significant ($P < 0.05$) or borderline

significant ($P \leq 0.10$) group differences were entered into Cox regression models using backward selection, with conversion to MCI as the outcome. Scores of cognitive subdomains were not included as predictors due to their strong association with the outcome. For the backward selection, all variables were z-transformed [(value-mean)/SD] to eliminate the influence of different measurement scales. The backward stepwise (conditional LR) method begins with all independent variables. It then iteratively removes the least significant variable (the one with the largest p-value) one step at a time, provided its p-value is above a certain threshold. The process ends when all remaining variables in the model are statistically significant, meaning no more variables can be removed without significantly harming the model's explanatory power. The final Cox regression model was then conducted with the selected variables that survived the backward selection. Results are reported as hazard ratios (HRs) with 95% confidence intervals (CIs) and P values. For the final model, maximally selected rank statistics identified optimal cut-off values for the raw continuous FW/DTI metrics. Model performance was evaluated using absolute χ^2 values, χ^2 change statistics, and P values for model improvement. To validate the result, we further conducted a comprehensive two-stage Cox proportional hazards modeling approach within a bootstrapping framework, beginning with backward stepwise elimination based on Akaike Information Criterion (AIC) to identify key predictors. For selected basal ganglia variables (FW values in GPe, GPi, putamen, caudate), optimal cut-points were determined using maximum log-rank statistics, converting these continuous measures to dichotomous variables. Bootstrap validation (1,000 iterations) was then performed to assess model optimism, with optimism-corrected C-index calculation and evaluation of variable selection stability. Following internal validation, coefficient shrinkage was applied using a bootstrap-based method that employed median coefficients from bootstrap samples, applying shrinkage factors constrained between 0.5 and 2.0 to correct for overfitting. C-index calculation, HR estimation, and graphical visualization were used to assess model performance.

Variance Inflation Factor (VIF) was also calculated to assess the multicollinearity of the final Cox model. A VIF value of 5 was set as the threshold for significant multicollinearity.

To identify the cognitive domains exhibiting the strongest associations with alterations in basal ganglia diffusion metrics and to explore potential biological underpinnings, Pearson correlation analyses were performed. These analyses assessed the relationships between the diffusion metrics and (1) cognitive subdomain scores, and (2) key biomarker levels, including serum NFL (reflecting neurodegeneration) and the CSF $A\beta_{42}$/pTau value.

The differential longitudinal difference of serum NFL between PD-MCI convertors and non-convertors was further investigated using a mixed linear model in PD patients, with time, group, and time×group interactive item as fixed effects and serum NFL as the outcome variable.

A two-tailed $P < 0.05$ defined statistical significance for all analyses.

Declarations

Availability of data and materials

PPMI data was publicly available on PPMI website (https://www.ppmi-info.org/).

Acknowledgements

The authors wish to acknowledge the helpful input and advice from Professors Tao Wu (Beijing Tiantan Hospital). PPMI – a public-private partnership – is funded by the Michael J. Fox Foundation for Parkinson's Research and funding partners, including 4D Pharma, Abbvie, AcureX, Allergan, Amathus Therapeutics, Aligning Science Across Parkinson's, AskBio, Avid Radiopharmaceuticals, BIAL, BioArctic, Biogen, Biohaven, BioLegend, BlueRock Therapeutics, Bristol-Myers Squibb, Calico Labs, Capsida Biotherapeutics, Celgene, Cerevel Therapeutics, Coave Therapeutics, DaCapo Brainscience, Denali, Edmond J. Safra Foundation, Eli Lilly, Gain Therapeutics, GE HealthCare, Genentech, GSK, Golub Capital, Handl Therapeutics, Insitro, Jazz Pharmaceuticals, Johnson & Johnson Innovative Medicine, Lundbeck, Merck, Meso Scale Discovery, Mission Therapeutics, Neurocrine Biosciences, Neuron23, Neuropore, Pfizer, Piramal, Prevail Therapeutics, Roche, Sanofi, Servier, Sun Pharma Advanced Research Company, Takeda, Teva, UCB, Vanqua Bio, Verily, Voyager Therapeutics, the Weston Family Foundation and Yumanity Therapeutics. Huimin Chen and Wen Su are funded by National High-Level Hospital Clinical Research Funding (BJ-2024-183, BJ-2023-067).

Authors' contributions

Study concept and design: WS, HbC, and HmC. Data analysis and interpretation: HmC. Drafting of the manuscript HmC. Critical revision of the manuscript for important intellectual content: all authors. Study supervision: WS and HbC. WS is the senior author, and took responsibility for the integrity of the data and the accuracy of the data analysis.

Competing interests

The authors declare no competing interests.

References

1 Baiano, C., Barone, P., Trojano, L. & Santangelo, G. Prevalence and clinical aspects of mild cognitive impairment in Parkinson's disease: A meta-analysis. Mov Disord. 35, 45-54 (2020).

2 Aarsland, D., Andersen, K., Larsen, J. P., Lolk, A. & Kragh-Sorensen, P. Prevalence and characteristics of dementia in Parkinson disease: an 8-year prospective study. Arch Neurol. 60, 387-392 (2003).

3 Schulz, J., Pagano, G., Fernandez Bonfante, J. A., Wilson, H. & Politis, M. Nucleus basalis of Meynert degeneration precedes and predicts cognitive impairment in Parkinson's disease. Brain 141, 1501-1516 (2018).

4 Slater, N. M., Melzer, T. R., Myall, D. J., Anderson, T. J. & Dalrymple-Alford, J. C. Cholinergic Basal Forebrain Integrity and Cognition in Parkinson's Disease: A Reappraisal of Magnetic Resonance Imaging Evidence. Mov Disord. 39, 2155-2172 (2024).

5 Crockett, R. A., Wilkins, K. B., Aditham, S. & Bronte-Stewart, H. M. No laughing white matter: Reduced integrity of the cortical cholinergic pathways in Parkinson's disease-related cognitive impairment. Neurobiol Dis. 185, 106243 (2023).

6 Sumra, V. et al. Regional free-water diffusion is more strongly related to neuroinflammation than neurodegeneration. J Neurol. 272, 478 (2025).

7 Ofori, E. et al. Increased free water in the substantia nigra of Parkinson's disease: a single-site and multi-site study. Neurobiol Aging 36, 1097-1104 (2015).

8 Ray, N. J. et al. Free-water imaging of the cholinergic basal forebrain and pedunculopontine nucleus in Parkinson's disease. Brain 146, 1053-1064 (2023).

9 Zhang, D. et al. Free-Water Imaging of the Nucleus Basalis of Meynert in Patients With Idiopathic REM Sleep Behavior Disorder and Parkinson Disease. Neurology 102, e209220 (2024).

10 Bohnen, N. I. et al. Frequency of cholinergic and caudate nucleus dopaminergic deficits across the predemented cognitive spectrum of Parkinson disease and evidence of interaction effects. JAMA Neurol. 72, 194-200 (2015).

11 Lee, B. et al. Dopaminergic modulation and dosage effects on brain state dynamics and working memory component processes in Parkinson's disease. Nat Commun. 16, 2433 (2025).

12 Siepel, F. J. et al. Cognitive executive impairment and dopaminergic deficits in de novo Parkinson's disease. Mov Disord. 29, 1802-1808 (2014).

13 Jia, X. et al. Differential functional dysconnectivity of caudate nucleus subdivisions in Parkinson's disease. Aging (Albany NY) 12, 16183-16194 (2020).

14 Gratwicke, J., Jahanshahi, M. & Foltynie, T. Parkinson's disease dementia: a neural networks perspective. Brain 138, 1454-1476 (2015).

15 Benarroch, E. What Are Current Concepts on the Functional Organization of the Globus Pallidus Externus and Its Potential Role in Parkinson Disease? Neurology 104, e213623 (2025).

16 Dong, J., Hawes, S., Wu, J., Le, W. & Cai, H. Connectivity and Functionality of the Globus Pallidus Externa Under Normal Conditions and Parkinson's Disease. Front Neural Circuits. 15, 645287 (2021).

17 Kubota, H., Zhou, X., Zhang, X., Watanabe, H. & Nagai, T. Pramipexole Hyperactivates the External Globus Pallidus and Impairs Decision-Making in a Mouse Model of Parkinson's Disease. Int J Mol Sci. 25 (2024).

18 Pedersen, K. F., Larsen, J. P., Tysnes, O. B. & Alves, G. Natural course of mild cognitive impairment in Parkinson disease: A 5-year population-based study. Neurology 88, 767-774 (2017).

19 Liu, Y. D. et al. Summary of the best evidence for non-pharmaceutical interventions for mild cognitive impairment in Parkinson's disease. Front Neurol. 16, 1598974 (2025).

20 Loetscher, T. Cognitive training interventions for dementia and mild cognitive impairment in Parkinson's disease - A cochrane review summary with commentary. NeuroRehabilitation 48, 385-387 (2021).

21 Mamikonyan, E., Xie, S. X., Melvin, E. & Weintraub, D. Rivastigmine for mild cognitive impairment in Parkinson disease: a placebo-controlled study. Mov Disord. 30, 912-918 (2015).

22 Weintraub, D. et al. Rasagiline for mild cognitive impairment in Parkinson's disease: A placebo-controlled trial. Mov Disord. 31, 709-714 (2016).

23 Masuda-Suzukake M. et al. Prion-like spreading of pathological α-synuclein in brain. Brain 136, 1128-1138 (2013).

24 Giovannoni F., Quintana F.J. The Role of Astrocytes in CNS Inflammation. Trends Immunol. 41, 805-819 (2020).

25 Barro, C., Chitnis, T. & Weiner, H. L. Blood neurofilament light: a critical review of its application to neurologic disease. Ann Clin Transl Neurol. 7, 2508-2523 (2020).

26 Kapoor, R. et al. Serum neurofilament light as a biomarker in progressive multiple sclerosis. Neurology 95, 436-444 (2020).

27 Turner, M. R., Thompson, A. G. & Teunissen, C. E. Blood level of neurofilament light chain as a biomarker for neurological disorders. BMJ Med. 4, e000958 (2025).

28 Aamodt, W. W. et al. Neurofilament Light Chain as a Biomarker for Cognitive Decline in Parkinson Disease. Mov Disord. 36, 2945-2950 (2021).

29 Batzu, L. et al. Plasma p-tau181, neurofilament light chain and association with cognition in Parkinson's disease. NPJ Parkinsons Dis. 8, 154 (2022).

30 Mitchell, T. et al. Neurite orientation dispersion and density imaging (NODDI) and free-water imaging in

Parkinsonism. Hum Brain Mapp. 40, 5094-5107 (2019).

31 Chen, H. et al. Perivascular space in Parkinson's disease: Association with CSF amyloid/tau and cognitive decline. Parkinsonism Relat Disord. 95, 70-76 (2022).

32 Irwin, D.J. et al. Evolution of Alzheimer's Disease Cerebrospinal Fluid Biomarkers in Early Parkinson's Disease. Ann Neurol. 88, 574-587 (2020).

33 Yu, L. et al. Plasma p-tau181 and p-tau217 in discriminating PART, AD and other key neuropathologies in older adults. Acta Neuropathol. 146, 1-11 (2023).

34 Ashton, N.J. et al. Diagnostic Accuracy of a Plasma Phosphorylated Tau 217 Immunoassay for Alzheimer Disease Pathology. JAMA Neurol. 81, 255-263 (2024).

35 Yuan Y.T., Hong W.P., Tan C.H. & Yu R.L. Influence of WWOX/MAF genes on cognitive performance in patients with Parkinson's disease. Neurobiol Di. 208, 106887 (2025).

36 Chahine L.M. et al. Modifiable vascular risk factors, white matter disease and cognition in early Parkinson's disease. Eur J Neurol. 26, 246-e18 (2019).

37 Guzzetti S., Mancini F., Caporali A., Manfredi L. & Daini R. The association of cognitive reserve with motor and cognitive functions for different stages of Parkinson's disease. Exp Gerontol. 115, 79-87 (2019).

38 Parkinson Progression Marker, I. The Parkinson Progression Marker Initiative (PPMI). Prog Neurobiol. 95, 629-635 (2011).

39 Litvan, I. et al. Diagnostic criteria for mild cognitive impairment in Parkinson's disease: Movement Disorder Society Task Force guidelines. Mov Disord. 27, 349-356 (2012).

40 Schrag, A., Siddiqui, U. F., Anastasiou, Z., Weintraub, D. & Schott, J. M. Clinical variables and biomarkers in prediction of cognitive impairment in patients with newly diagnosed Parkinson's disease: a cohort study.

Lancet Neurol. 16, 66-75 (2017).

41 Chen, F. et al. Development and Validation of a Prognostic Model for Cognitive Impairment in Parkinson's Disease With REM Sleep Behavior Disorder. Front Aging Neurosci. 13, 703158 (2021).

42 Mollenhauer, B. et al. Validation of Serum Neurofilament Light Chain as a Biomarker of Parkinson's Disease Progression. Mov Disord. 35, 1999-2008 (2020).

43 Tournier, J. D. et al. MRtrix3: A fast, flexible and open software framework for medical image processing and visualisation. Neuroimage 202, 116137 (2019).

44 Pasternak, O., Sochen, N., Gur, Y., Intrator, N. & Assaf, Y. Free water elimination and mapping from diffusion MRI. Magn Reson Med. 62, 717-730 (2009).

Figure Captions

Fig. 1 Comparison of FW within basal ganglia between groups

PD-MCI convertors had higher FW in the GPi compared with non-convertors and HC, and higher FW in GPe and caudate compared with HC. PD-MCI non-convertors also had higher FW in the putamen and GPi than HC. Only a significant group difference was indicated with LSD corrected P value.

Fig. 2 Predictive value of GPe FW for PD-MCI conversion

a Density distribution of GPe FW values across study groups. The curve illustrated a bimodal pattern distinguishing high-risk (red) and low-risk (cyan) subgroups. **b** Maximally selected rank statistics identified the optimal cut-point (0.328, dashed line) for stratifying MCI conversion risk based on GPe FW. Red and blue dots represented subjects above and below the threshold, respectively. **c** Kaplan–Meier curves showed cumulative MCI conversion probability over five years. Patients with GPe FW > 0.328 (red curve) had a significantly higher risk of conversion than those with GPe FW < 0.328.

Fig. 3 Correlation of GPe FW with executive function and biomarkers

a GPe FW value showed significant negative correlations with attention/working memory (assessed by the Letter Number Sequencing test) and processing speed (assessed by the Symbol Digit Modalities test); these correlations were absent in HC. **b** GPe FW was significantly positively correlated with serum NFL level, specifically in the PD group, but not with CSF $A\beta_{42}$/pTau levels in either group.

Fig. 4 Plotting of longitudinal serum NFL levels by visit and groups

Data points represented mean values with error bars indicating standard deviation. PD-MCI convertors showed consistently elevated serum NFL levels compared with non-convertors and HC, with an increasing trend over time. Serum NFL level in the fourth year was not available in the dataset.

Table 1. Group comparison of baseline demographic and behavioral variables

	PD-MCI convertor (n =30)	PD-MCI Non-convertor	HC (n = 100)	P value	Post hoc (LSD corrected) P value		
					PD-MCI convertor vs. PD-MCI Non-convertor	PD-MCI convertor vs. HC	PD-MCI Non-convertor vs. HC

		(n =82)			convertor vs. non-convertor	convertor vs. HC	non-convertor vs. HC
Age, years, median (IQR)	64.95 (57.23–70.98)	60.47 (51.93–69.26)	64.59 (56.39–70.76)	0.081	/	/	/
Gender (female/male)	13/17	32/50	47/53	0.558	/	/	/
Education, years, median (IQR)	16 (12–18)	16 (14–18)	16 (13–18)	0.172	/	/	/
Disease duration, months, median (IQR)	6.02 (3.19–111.13)	3.67 (2.57–6.67)	/	0.154	/	/	/
Hoehn-Yahr stage, median (IQR)	2 (1–2)	2 (1–2)	0 (0–0)	**<0.001*****	**0.025***	**<0.001*****	**<0.001*****
MDS-UDPRS part I score,	5 (2–8)	4 (2–6)	2 (0–4)	**<0.001*****	**0.021***	**<0.001*****	**0.015***

median (IQR)							
MDS-UPDRS part II score, median (IQR)	4 (2–9)	3 (2–6)	0 (0–0)	**<0.001*****	0.283	**<0.001*****	**<0.001*****
MDS-UPDRS part III score, median (IQR)	22 (16–26)	17.5 (12–26)	0 (0–2)	**<0.001*****	**0.013***	**<0.001*****	**<0.001*****
MDS-UPDRS total score, median (IQR)	33 (23–42)	27 (17–38)	3 (1–7)	**<0.001*****	**0.006****	**<0.001*****	**<0.001*****
Geriatric Depression Scale score, median (IQR)	2 (1–4)	1 (0–3)	1 (0–2)	**0.002****	0.117	**0.017***	0.275
State Trait Anxiety Index score, median (IQR)	65 (50–78)	58.5 (51–70)	50 (45–63)	**<0.001*****	0.162	**0.001****	**0.010***
Epworth Sleepiness	6 (5–9)	5 (3–7)	5 (3–8)	0.131	/	/	/

Scale score, median (IQR)							
University of Pennsylvania Smell Identification Test score, median (IQR)	21 (15–26)	24 (17–30)	33 (30–37)	**<0.001*****	**0.036***	**<0.001*****	**<0.001*****
RBD Screening Questionnaire score, median (IQR)	3 (2–5)	3 (2–5)	2 (1–4)	**0.010***	0.748	0.114	**0.008****
Questionnaire for Impulsive-Compulsive Disorders score, median (IQR)	0 (0–1)	0 (0–0)	0 (0–0)	0.216	/	/	/
Scale for Outcomes in	8 (5–12)	7 (4–11)	6 (4–9)	**0.012****	0.254	**0.013***	0.064

Parkinson's disease-Autonomic score, median (IQR)							
Montreal Cognitive Assessment score (education adjusted), median (IQR)	28 (26–29)	28 (27–29)	28 (27–29)	0.779	/	/	/
HVLT Total Recall, median (IQR)	24 (21–27)	27 (23–30)	26 (23–30)	0.143	**0.028***	0.096	0.405
HVLT Recognition Discrimination, median (IQR)	10 (9–11)	11 (9–12)	11 (10–12)	**0.045***	0.063	0.132	0.575
Benton	12 (11–14)	14 (12–15)	14 (13–14)	**0.006****	**0.003****	**0.002****	0.882

Judgment of Line Orientation, median (IQR)							
Symbol Digit Modalities, median (IQR)	39 (32–46)	43 (38–50)	46 (40–52)	**0.006****	0.109	**0.003****	0.051
Letter Number Sequencing, median (IQR)	10 (9–12)	11 (10–13)	11 (9–13)	0.416	/	/	/
Semantic Fluency Test (animal), median (IQR)	19 (16–22)	22 (19–26)	20 (19–25)	**0.002****	**0.001****	**0.002****	0.732

Abbreviations: IQR, interquartile range; MCI, mild cognitive impairment; MDS-UPDRS, Movement Disorder Society Unified Parkinson's Disease Rating Score; RBD, Rapid eye movement sleep Behavior Disorder; SD, standard deviation.

Table 2. Group comparison of baseline imaging and biochemical variables

	PD-MCI convertor (n =30)	PD-MCI Non-convertor (n =82)	HC (n = 100)	P value	Post hoc P value		
					PD-MCI convertor vs. non-convertor	PD-MCI convertor vs. HC	PD-MCI non-convertor vs. HC
Mean DAT caudate uptake, mean±SD	1.78±0.52	1.93±0.49	2.82±0.48	**<0.001*****	0.231	**<0.001*****	**<0.001*****
Mean DAT putamen uptake, mean±SD	0.81±0.32	0.82±0.24	2.04±0.42	**<0.001*****	0.923	**<0.001*****	**<0.001*****
CSF $A\beta_{42}$ level, pg/mL, median (IQR)	766.60 (617.18–894.13)	763.15 (575.99–1014.75)	811.05 (649.65–1047.00)	0.703	/	/	/
CSF α-syn level, pg/mL,	1448.45 (1203.13–	1390.65 (1029.65–	11522.00 (1036.80–	0.563	/	/	/

median (IQR)	19774.38)	1838.73)	1966.30)				
CSF tTau, median (IQR)	150.25 (135.53–213.00)	157.40 (125.43–205.45)	166.40 (127.65–205.03)	0.859	/	/	/
CSF pTau, median (IQR)	13.07 (11.40–18.70)	13.23 (10.86–17.28)	14.70 (11.11–19.66)	0.438	/	/	/
CSF $A\beta_{42}$/tTau, median (IQR)	4.770 (4.228–6.08)	5.46 (4.33–6.39)	5.74 (4.50–6.22)	0.235	/	/	/
CSF $A\beta_{42}$/pTau, median (IQR)	59.46 (47.80–69.31)	66.95 (51.38–78.13)	66.10 (56.29–77.46)	0.100	0.057	0.090	0.898
Serum NFL, pg/mL, median (IQR)	12.70 (9.19–17.20)	10.90 (7.60–15.80)	11.00 (7.95–13.70)	0.140	/	/	/
Putamen FW, mean±SD	0.317±0.023	0.307±0.026	0.298±0.027	**<0.001*****	0.062	**<0.001*****	**0.003****
Caudate FW, mean±SD	0.446±0.034	0.438±0.046	0.432±0.039	**0.150**	0.351	0.068	0.220

GPe mean±SD	FW,	0.328±0.030	0.316±0.022	0.317±0.050	**0.032***	0.057	**0.009****	0.344
GPi mean±SD	FW,	0.340±0.031	0.328±0.022	0.320±0.043	**<0.001*****	**0.038***	**<0.001*****	**0.003****

Abbreviations: CSF, cerebrospinal fluid; DAT, dopaminergic transporter; FW, free water; GPe, external globus pallidus; GPi, internal globus pallidus; IQR, interquartile range; NFL, neurofilament light chain; SD, standard deviation.

Table 3. Cox regression models

	HR (95% CI)	P value
Mode 1		
MDS-UPDRS part I score	1.146 (1.045–1.257)	**0.004****
CSF $A\beta_{42}$/pTau ratio	0.975 (0.956–0.995)	**0.016***
Model 2		
MDS-UPDRS part I score	1.224 (1.108–1.353)	**<0.001*****
CSF $A\beta_{42}$/pTau ratio	0.966 (0.946–0.986)	**0.004****
GPe FW value<0.328 (N = 86)	REF	REF
GPe FW value>0.328 (N = 26)	4.698 (1.974–11.179)	**<0.001*****
	Improved χ^2 = 11.205	**P *for improvement* = 0.001****
Model 3		
MDS-UPDRS part I score	1.2458 (1.124–1.389)	**<0.001*****
CSF $A\beta_{42}$/pTau ratio	0.9612 (0.944–0.987)	**0.002****
GPe FW value<0.328 (N = 86)	REF	REF
GPe FW value>0.328 (N = 26)	4.7571 (1.330–17.016)	0.017*
Study site	0.966 (0.814–1.146)	0.690
Site × GPe FW value	1.119 (0.814–1.900)	0.678
	Improved χ^2 = 0.165	P *for improvement* = 0.921

All variables entered the models simultaneously.

Abbreviations: CI, confidence interval; CSF, cerebrospinal fluid; FW, free water; GPe, external globus pallidus;

HR, hazard ratio; MDS-UPDRS, Movement Disorder Society Unified Parkinson's Disease Rating Score.

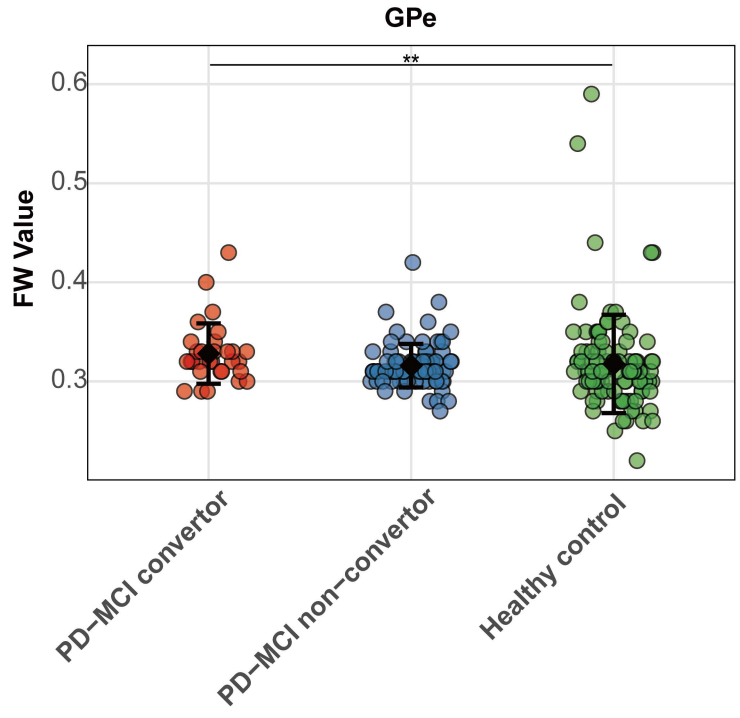
GPe
FW Value
0.6
0.5
0.4
0.3
**
PD−MCI convertor
PD−MCI non−convertor
Healthy control

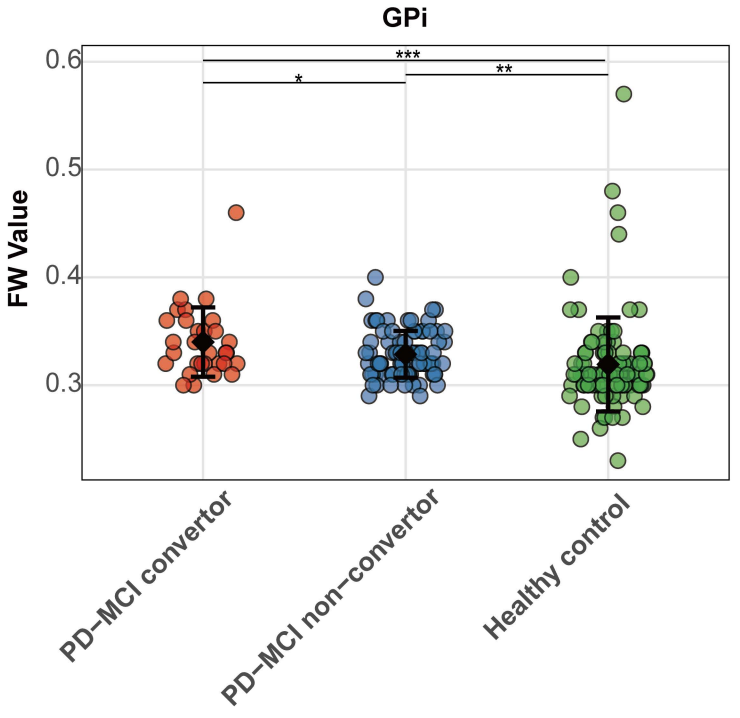
GPi
FW Value
0.6
0.5
0.4
0.3
***
**
*
PD−MCI convertor
PD−MCI non−convertor
Healthy control

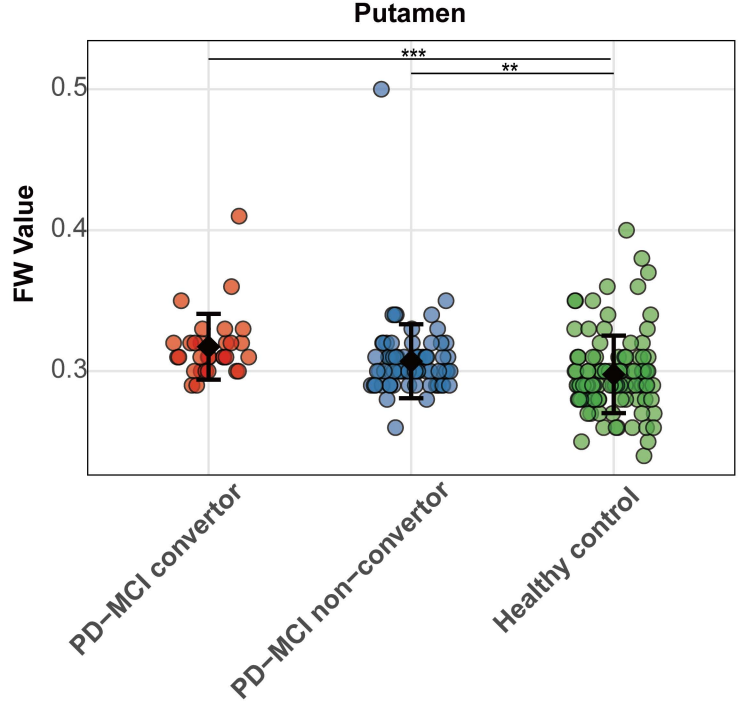
Putamen
FW Value
0.5
0.4
0.3
***
**
PD−MCI convertor
PD−MCI non−convertor
Healthy control

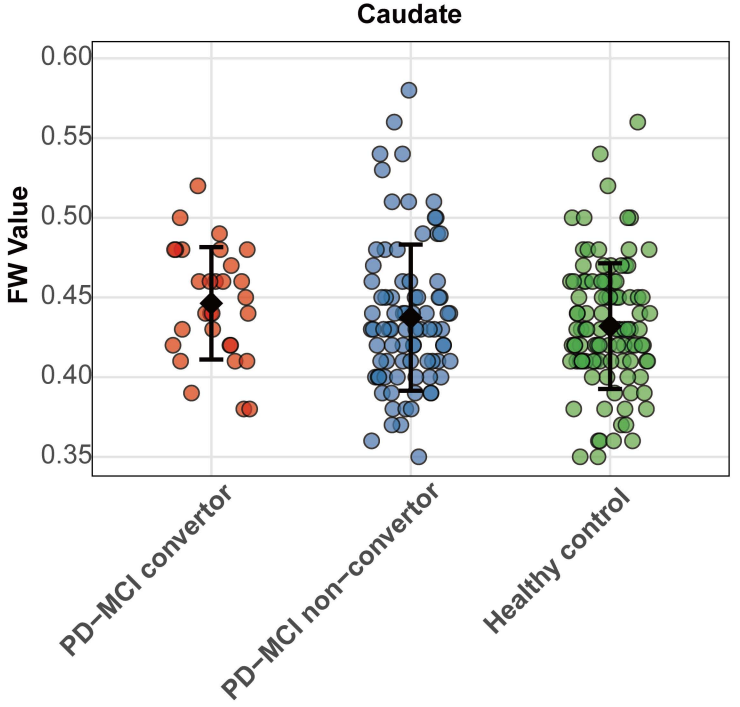
Caudate
FW Value
0.60
0.55
0.50
0.45
0.40
0.35
PD−MCI convertor
PD−MCI non−convertor
Healthy control

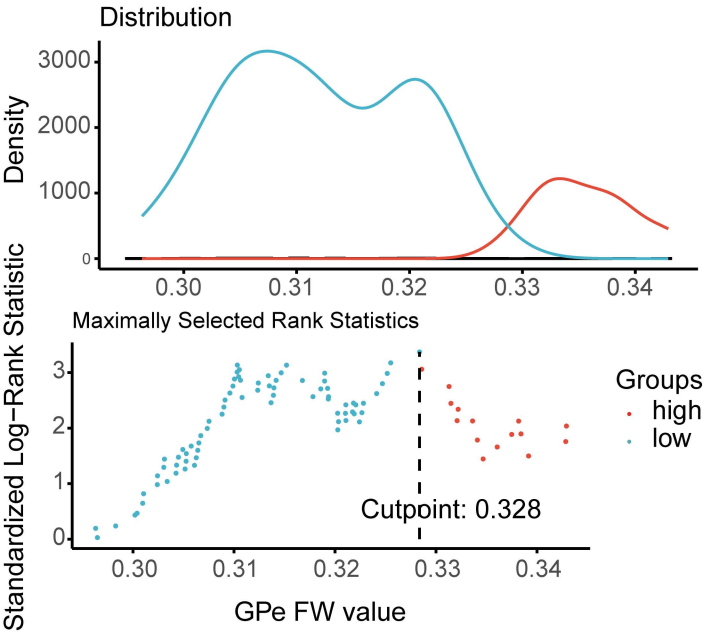

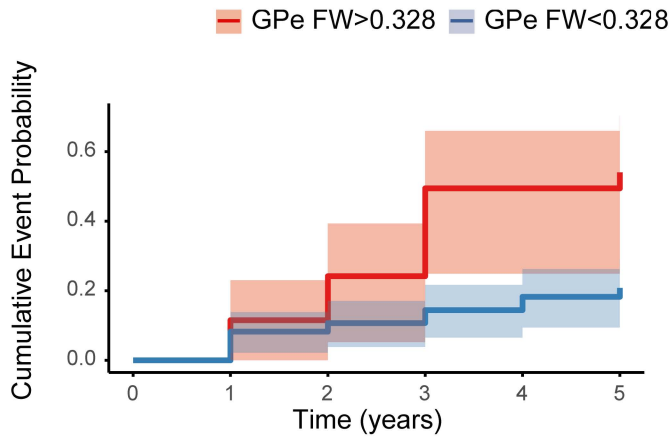

Number at risk

GPe FW>0.328	27	26	21	18	11	11
GPe FW<0.328	85	85	74	72	67	64
	0	1	2	3	4	5

Time (years)

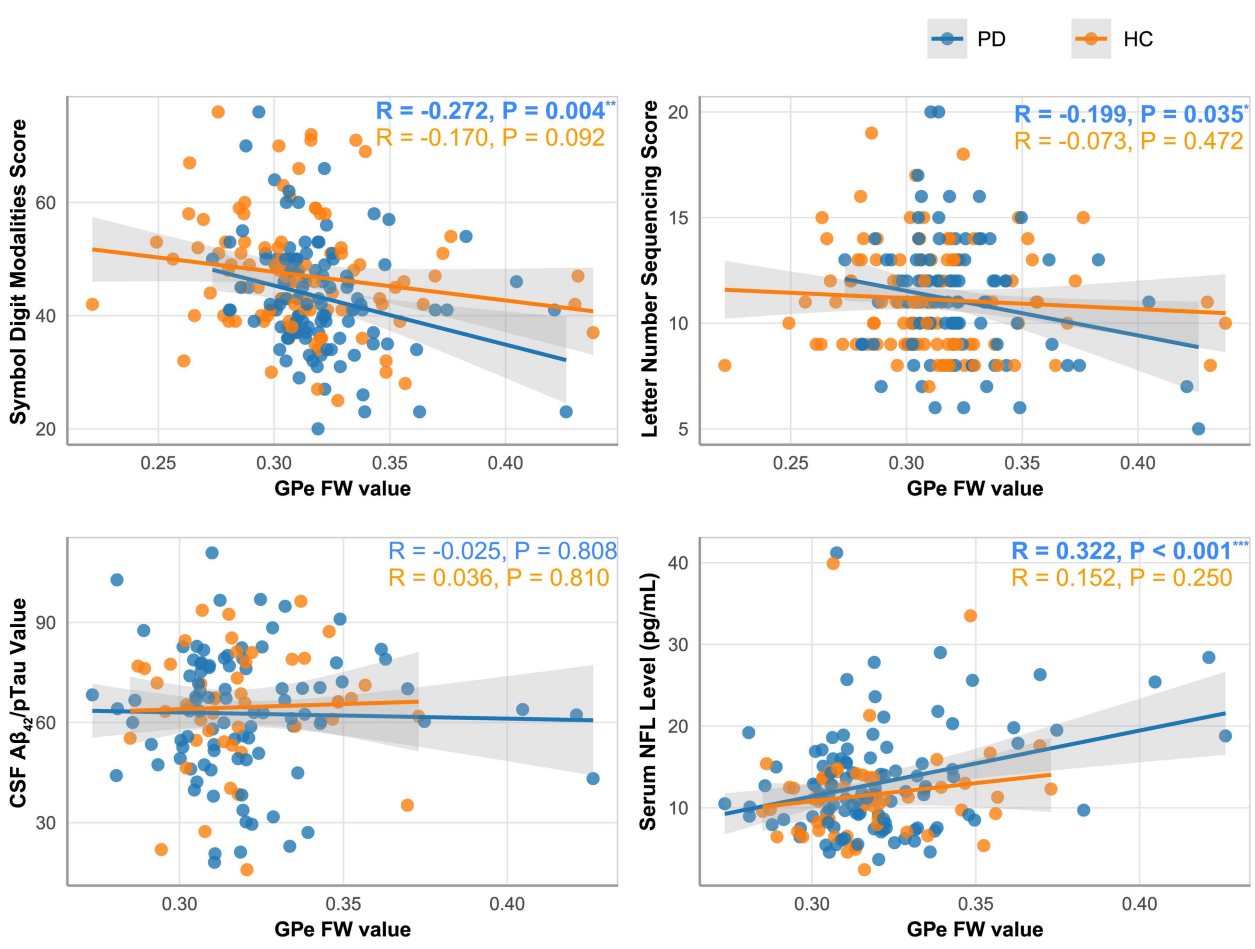
PD
HC
R = -0.272, P = 0.004**
R = -0.170, P = 0.092
Symbol Digit Modalities Score
GPe FW value
R = -0.199, P = 0.035*
R = -0.073, P = 0.472
Letter Number Sequencing Score
GPe FW value
R = -0.025, P = 0.808
R = 0.036, P = 0.810
CSF Aβ42/pTau Value
GPe FW value
R = 0.322, P < 0.001***
R = 0.152, P = 0.250
Serum NFL Level (pg/mL)
GPe FW value